Korean J. Chem. Eng., **31**(6), 1057-1064 (2014)
DOI: 10.1007/s11814-014-0018-2

pISSN: 0256-1115
eISSN: 1975-7220

Preparation, characterization and performance of cellulose acetate ultrafiltration membranes modified by charged surface modifying macromolecule

Palsamy Kanagaraj, Sivasubramaniyan Neelakandan, and Alagumalai Nagendran†

Polymeric Materials Research Lab., PG & Research Department of Chemistry,
Alagappa Government Arts College, Karaikudi - 630 003, India
(*Received 12 November 2013 • accepted 12 January 2014*)

Abstract−A charged surface modifying macromolecule (cSMM) was synthesized, characterized by FT-IR spectroscopy and blended into the casting solution of cellulose acetate (CA) to prepare surface modified UF membranes by phase inversion technique. With an increasing cSMM additive content from 1 to 4 wt%, pure water flux (PWF) and water content (WC) were increases whereas the hydraulic resistance decreases. Surface characteristic study reveals that the surface hydrophilicity increased in cSMM modified CA membranes. The pore size and surface porosity of the 4 wt% cSMM blend CA membranes increases to 41.26 Å and 0.015%, respectively. Similarly, the molecular weight cut-off (MWCO) of the membranes ranged from 20 to 45 kDa, depending on the various compositions of the prepared membranes. Lower flux decline rate (47.2%) and higher flux recovery ratio (FRR) (89.0%), exhibited by 4 wt% cSMM blend membranes demonstrated its fouling resistant characteristic compared to pristine CA membrane.

Keywords: Cellulose Acetate, cSMM, Ultrafiltration, Phase Inversion Technique, Membrane Antifouling

INTRODUCTION

Membranes have gained an important place in chemical engineering and technology and are used in a variety of applications. Membrane technology is widely applied for water treatment and is an outstanding process for the removal of particles, turbidity and microorganisms of natural and waste water [1,2]. Especially microfiltration (MF) and UF membranes have been getting more and more application in the field of separation process associated with their advantages including superior water easier control of operation, lower cost and maintenance [3-5].

The asymmetric membranes used in UF are usually made from polymers such as CA, poly (ether sulfone) (PES), poly (ether imide) (PEI) and poly sulfone (Psf) etc. CA is one of the first polymer membranes that have been used for aqueous based separation, i.e., reverse osmosis and UF techniques [6]. CA, an environment-friendly product from sustainable resources became an interesting polymer with regard to its low price, moderate chlorine resistance, good biocompatibility and hydrophilicity [7]. However, CA is not suitable for more aggressive cleaning as it has low oxidation and chemical resistances and poor mechanical strength. Hence modification of CA gains importance [8].

The performance of CA may be improved by mixing it with appropriate additives to fulfill new requirements and associated membrane properties. Phase separation is one of the most popular methods used to produce porous polymeric membranes. Usually, a hydrophilic polymer additive is blended with the membrane forming ability polymer to obtain hydrophilic membranes. Several researches have reported on the role of additives in the membrane structures. Some additives have the tendency to form macrovoids, others help in suppressing the macrovoids, improving interconnectivity of the pores and resulting in higher porosities in the top layer and the sub layer. Yeo et al. using poly (vinylpyrrolidone) (PVP) in the casting solution of PSf and N, N′-dimethyl formamide (DMF) indicated the enlargement of the macrovoid structure in the prepared membranes rather than the suppression of that structure [9]. Study of Jimenez et al. using PVP as additive on PES membranes showed that the addition of PVP increased the MWCO and pure water permeation of the PES membranes [10]. Nagendran et al. studied the surface modification of CA/PEI blend membranes using pore forming polymeric additive poly ethylene glycol (PEG) as one of the components in the UF membrane casting solution [11].

Blending polymers with hydrophilic functional groups is one of the methods of surface modification [12-15]. Currently, many researchers have attempted the modification of base polymer by blending surface modifying macromolecules (SMMs) [16-19]. SMM is a simple blending method which uses the idea of surface segregation in polymer science as detailed elsewhere [20,21]. SMM when introduced as an additive in a base polymer will migrate to the surface and change the chemistry of the surface while maintaining its bulk properties. The bulk properties remain almost unchanged, for a very small amount of SMM additive is needed to cover the membrane surface completely [22-24].

Hamza et al. reported that SMMs blended PES membranes were less susceptible to fouling in oil-water separation [25]. They also suggested that SMMs blended membranes might be useful for other water treatment processes as membranes with high fouling resistance. PES hollow fiber NF membranes have been developed by blending negatively charged cSMM for the removal of bisphenol A from wastewater [26]. Rana et al. used hydrophilic SMM in producing hydrophilic PES - UF membranes with high fouling resistance [17].

†To whom correspondence should be addressed.
E-mail: nagimmm@yahoo.com

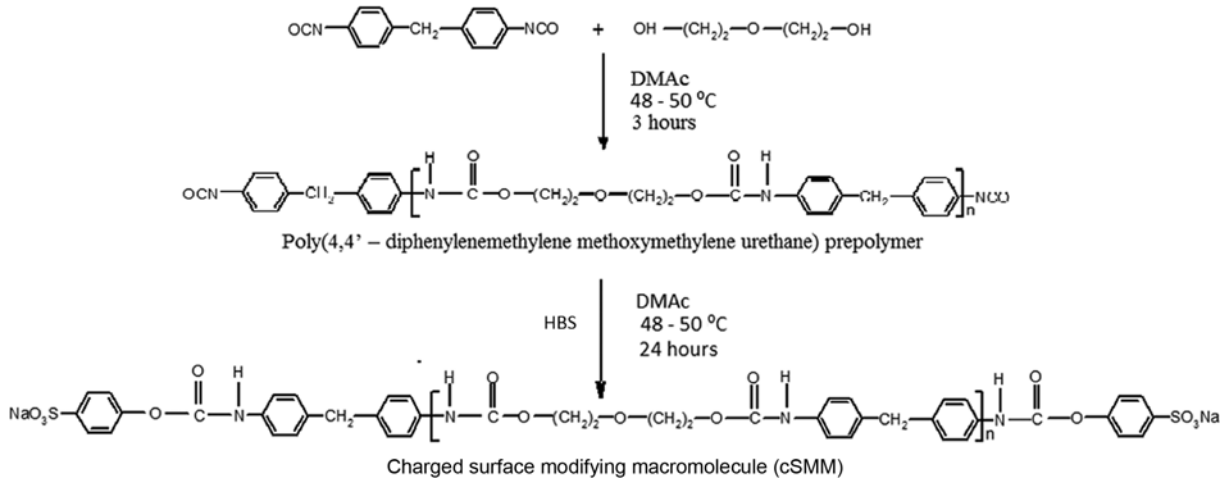

Fig. 1. Scheme of the chemical reaction for synthesis of cSMM.

In this present investigation, cSMM was synthesized and blended with the polymer of CA by phase inversion technique in various compositions. All the prepared membranes were subjected to UF characterizations such as membrane compaction, PWF, membrane hydraulic resistance, pore size, surface porosity, MWCO, protein permeate flux and surface characterization. Fouling evaluation of pure CA and CA/cSMM blend membranes were studied by flux decline rate, FRR, surface fouling and internal membrane fouling.

EXPERIMENTAL

1. Materials

CA (CA-398-30) was received as a gift sample from Eastman Chemical Company, Mumbai, India. CA was re-crystallized from acetone and then dried in a vacuum oven at 70 °C for 24 h prior to use. Dimethylacetamide (DMAc), methylene bis para phenyl isocyanate (MDI), DEG, N-methyl-2-pyrrolidone (NMP), hydroxyl benzene sulfonate (HBS), bovine serum albumin (BSA) (69 kDa), egg albumin (EA) (45 kDa), pepsin (35 kDa), trypsin (20 kDa) and sodium lauryl sulphate (SLS) of analar grades were procured from Sigma Aldrich (USA). Anhydrous sodium monobasic phosphate and sodium dibasic phosphate heptahydrate were also procured from Sigma Aldrich (USA) and used for the preparation of phosphate buffer solutions in the protein analysis. All chemicals were used as such without further purification. De-ionized and distilled water was employed for the UF experiments and for the preparation of the membranes.

2. Synthesis of Charged Surface Modifying Macromolecule

The cSMM synthesis was done according to the procedure reported by Mohd Norddin et al. [27]. The cSMM, endcapped with hydroxyl sulfonate, was synthesized using a two-step solution polymerization method. The first step involved the reaction of MDI with DEG in a common solvent of DMAc. This mixture formed a urethane prepolymer solution. The prepolymer is a segment-blocked urethane oligomer, poly (4,4′-diphenylenemethylene methoxymethylene urethane) having both endcapped with isocyanate. The reaction was then terminated by the addition of HBS resulting in a solution of charged or sulfonated SMM. Detailed procedure: The effect of moisture was removed by drying all glassware overnight at 110 °C and the polymerization reaction was performed in a controlled condition. To a solution of 0.03 mol MDI (7.5 g) in 50 ml of degassed DMAc was loaded in a 1-L Pyrex round bottom flask. Then, a solution of 0.02 mol degassed DEG (2.122 g) in 100 ml of degassed DMAc was added dropwise with stirring to react for 3 hours. Then 0.02 mol of HBS (4.644 g) dissolved in 50 ml of degassed DMAc was added dropwise and the solution was left under stirring for 24 h at 48-50 °C, resulting in a solution of cSMM. The reaction scheme of the cSMM is listed in Fig. 1. The cSMM solution was added dropwise into a beaker filled with distilled water under vigorous stirring to precipitate the cSMM. Prepared cSMM was kept immersed in distilled water for 24 h under stirring to leach out residual solvent. They were then dried in an air circulation oven at 50 °C for 5 days and stored in a glass bottle.

3. Characterization of cSMM by FT-IR

Fourier transforms infrared spectroscopy (FT-IR) was used to observe the presence of funtional groups in cSMM. The data were collected on an FT-IR spectrometer (TENSOR 27, Bruker optik GmbH, Germany). The spectra were measured in absorbance mode over a wave numbers range of 370 to 4,000 cm^{-1}.

4. Membrane Preparation

The phase inversion technique was employed to prepare membranes [28]. The casting environment (relative humidity and temperature) was standardized for the preparation of membranes with better physical properties such as the homogeneity, thickness, and smoothness. The membrane-casting chamber was maintained at a temperature of 24±1 °C and a relative humidity of 50±2%. The total polymer concentration was maintained at 17.5 wt% in order to have a balanced casting solution viscosity to yield membranes between a spongy type and a high macrovoidal type. The casting and gelation conditions were maintained constant throughout because the thermodynamic conditions would largely affect the morphology and performance of the resulting membranes [29].

5. Membrane Characterization

The prepared membranes were cut into the required size for use in the UF cell (Amicon 8400-Model, Millipore, USA) fitted with a Teflon-coated magnetic paddle. The effective membrane area available for UF was 0.00385 m^2. The solution filled in the cell was stirred at 300 rpm using a magnetic stirrer. All the experiments were at

30±2 °C.

6. Membrane Compaction

Before using a fresh membrane, it was compacted with de-ionized water for 5 h at a trans-membrane pressure (TMP) of 414 kPa, which is higher than the maximum operating pressure in the present study. The water flux was calculated from the experimental permeate flow rate measured at every 1 h interval after attaining steady state flux value. PWF was calculated over measured time intervals using the following equation [30].

$$J_w = \frac{Q}{A\Delta t} \quad (1)$$

where Q is the quantity of permeate collected (in *l*), J_w is the water flux ($lm^{-2}h^{-1}$), Δt is the sampling time (in h), and A is the membrane area (in m^2).

7. Pure Water Flux and Hydraulic Resistance Study

PWF of different membranes, after compaction study, was calculated at different TMPs (ΔP) ranging from 345 kPa to 69 kPa, using Eq. (1). To determine the hydraulic resistance (R_m) of the membrane, the PWF of the membranes were measured at TMPs (ΔP) of 69, 138, 206, 275, and 345 kPa, respectively, after compaction. The resistance of the membrane, R_m was evaluated from the slope of PWF versus TMP difference (ΔP) using the following equation [31].

$$J_w = \frac{\Delta P}{R_m} \quad (2)$$

8. Water Content Measurement

WC is related to the hydrophilicity or hydrophobicity of membranes. Membrane samples were cut into desired size and soaked in water for 24 h and weighed immediately after blotting the free surface water. These wet membranes were dried for 48 h at 75± 58 °C and the dry weights were determined. From these values, the percentage of water contents were calculated as follows [32].

$$\%WC = \left(\frac{W_w - W_d}{W_w}\right) \times 100 \quad (3)$$

where W_w and W_d are the weight of the wet and the dry membranes, respectively.

9. Molecular Weight Cut-off and Proteins Permeate Flux

MWCO is a pore characteristic of membranes and is related to rejection for a given molecular weight of a solute. The MWCO has a linear relationship with the pore size of the membrane [33]. In this study proteins of different molecular weight such as BSA (69 kDa), EA (45 kDa), pepsin (35 kDa) and trypsin (20 kDa) were chosen for the estimation of MWCO. The studied protein solution was prepared at a concentration of 0.1 wt% in phosphate buffer (pH= 7.2) solution. The permeate protein concentration was estimated by using UV-visible double beam spectrophotometer (Systronics, 2201) at a wavelength of 280 nm. The percentage solute rejection (SR) was calculated from the concentration of the feed and the permeate using the following equation [34].

$$\%SR = \left(1 - \frac{C_p}{C_f}\right) \times 100 \quad (4)$$

where C_p and C_f are the concentrations of permeate and feed solutions, respectively, and also proteins permeate flux is determined by using Eq. (1).

10. Scanning Electron Microscopy Measurement

The top surface morphologies of the pure CA and CA/cSMM blend membranes were studied by scanning electron microscopy (SEM) (HRSEM, FEI Quanta 250 Microscope, and Netherland) under vacuum conditions. Sample was gold-sputtered prior to SEM analysis.

11. Contact Angle and Adhesion Work Measurement

The hydrophilicity of the surface was evaluated based on the water contact angle (θ) of the membrane, which was measured using a contact angle **(**NIMA DST 9005 Dynamic Surface Tensiometer). From values of the contact angle, the adhesion work ω_A (surface energy) necessary to pull water from a square meter of membrane surface can be calculated by the following equation [35].

$$\omega_A = \gamma_w(1+\cos\theta) \quad (5)$$

where, γ_w is surface tension of water (7.2×10^{-2} N/m) and (θ) is the contact angle.

12. Average Pore Size and Porosity Measurement

The average pore size and surface porosity of the membranes were determined by the UF of protein solutions of different molecular weights. The molecular weight of the solute, which has solute rejection (SR) above 80%, may be used to evaluate the average pore size, of the membranes by the following equation.

$$\overline{R} = 100\left(\frac{\alpha}{\%SR}\right) \quad (6)$$

where $\overline{R}$ is the average pore size (radius) of the membrane (Å), and α is the average solute radius (Å). The average solute radii, also known as the Stoke radii, were obtained from the plot of solute molecular weight versus solute radius in aqueous solution, which was developed by Sarbolouki [36].

The surface porosity or percentage porosity ε, of the membrane can be calculated by the following "orifice model" and assuming membrane as asymmetric skin type, using following equation [37].

$$\varepsilon = \frac{3\pi\mu J_w}{\Delta P\overline{R}} \quad (7)$$

where μ is the viscosity of the permeate water in (Pa s); J_w, the PWF of the membrane in ($m^3m^{-2}s$); $\overline{R}$, the average pore radius in (Å); and ΔP is the TMP in (Pa).

13. Fouling Studies

The prepared pure CA membrane and surface modified CA blend membranes were subjected to fouling resistant studies by means of flux decline rate, FRR and fouling reversibility.

13-1. Flux Decline Rate

0.1 wt% of BSA solution was prepared in phosphate buffer solution (pH=7.2) and used as feed solution for the fouling studies. Each membrane was initially compacted for 30 min and the PWF, Jw_1 was measured at a TMP of 345 kPa. The initial protein permeate flux, Jp_1 and steady state protein flux, Jp after 4 h of filtration were recorded. The flux decline rate of pure CA and CA/cSMM blend membranes was calculated by the following equation.

$$R_{fd} = \left[1 - \left(\frac{J_p}{J_{w_1}}\right)\right] \times 100 \quad (8)$$

13-2. Flux Recovery Ratio

After UF of the BSA solution study, the fouled membrane was

washed with deionized water for 30 min. The PWF of the cleaned membranes was measured again under the same conditions (now denoted as Jw_2). To measure fouling resistant ability of membranes, the FRR was introduced and calculated by the following equation [38].

$$FRR = \left[\frac{J_{w_2}}{J_{w_1}}\right] \times 100 \quad (9)$$

13-3. Surface Fouling and Internal Membrane Fouling

Surface fouling is the deposition of retained colloidal and macromolecular materials on the membrane surface. It can be removed by backwashing and using hydrophilic or charged membranes. Generally, surface fouling is reversible, which can be calculated using the following equation [39].

$$R_r = \left[\frac{J_{w_2} - J_p}{J_{w_1}}\right] \times 100 \quad (10)$$

Internal fouling is caused by penetration of solid material into the inner surface of membranes, which results in pore blocking. Internal membrane fouling is generally irreversible [40]. It cannot be removed by backwashing and it can be calculated using the following equation:

$$R_{ir} = \left[\frac{J_{w_1} - J_{w_2}}{J_{w_1}}\right] \times 100 \quad (11)$$

RESULTS AND DISCUSSION

1. Characterization of cSMM by FT-IR Spectra

The structure of the synthesized material is confirmed by FT-IR technique. The FT-IR spectrum of cSMM shows that the presence of sulfonic groups in cSMM can be confirmed by the absorption bands at 3,336 cm^{-1} (O-H), 1,230 cm^{-1} (asymmetric O=S=O), 1,068 cm^{-1} (symmetric O=S=O), 1,018 cm^{-1} (S=O) and 700 cm^{-1} (S-O) and sulfonic group stretching vibration at 1,407 cm^{-1} (Fig. 2), and presence of absorption band at 1,662 cm^{-1}, which corresponds to amide C=O stretch. The absorption band noted at 1,229 cm^{-1} indicates Ph-O-C and the appearance of CH_2 asymmetric and C-O-C asymmetrical stretching is confirmed by the absorption band noted at 2,910 cm^{-1} and 1,308 cm^{-1} and the aromatic bands at 1,541 and 1,510 cm^{-1}.

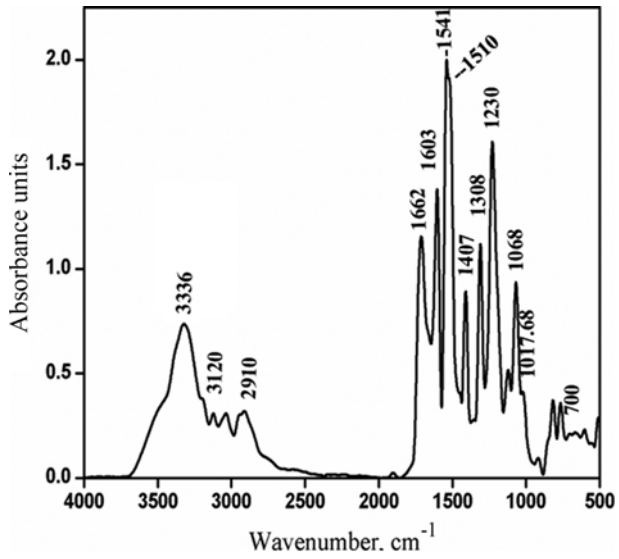

Fig. 2. The FT-IR spectrum of cSMM.

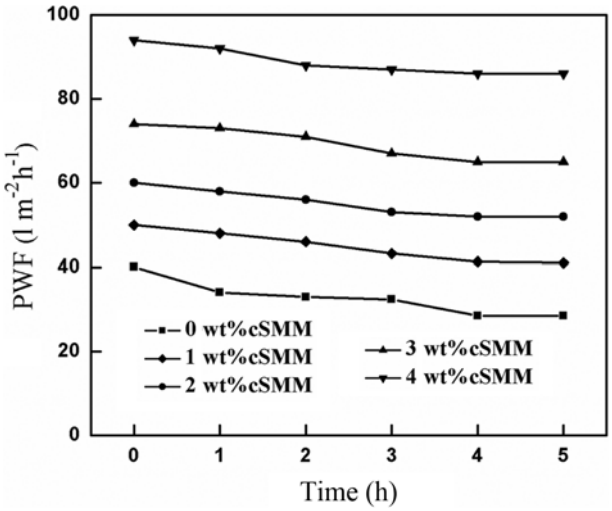

Fig. 3. The effect of compaction time on pure water flux of CA/cSMM blend membranes at 60 psi.

2. Effect of Compaction Time on Flux

Compaction is defined as a compression of the membrane structure under a TMP difference causing a decrease in membrane permeability [41,42]. The prepared blend membranes were subjected to hydraulic compaction at 414 kPa TMP. The compaction was carried out for 5 h under stirred conditions to attain steady-state flux and the water flux measured at every 1 h. The PWF on compaction at every 1 h for all CA and CA/cSMM membranes is reported in Fig. 3. From the figure, it has been observed that in the case of pure CA membrane, PWF decreased from 40.10 to 28.50 $lm^{-2}h^{-1}$ with an increasing time of compaction and almost remained constant, after a definite time of 5 h, indicating the completion of compaction. In case of CA/cSMM blend membrane, an increase in the blend polymer solution 1 to 4 wt% of total polymer increased the flux from 50 to 94 $lm^{-2}h^{-1}$. This increase in flux upon increase in cSMM additive concentration may be due to the increase in hydrophilic nature of blend membrane. In all CA/cSMM modified blend membranes, the initial PWF was increased and finally attained the steady state flux value.

3. Effect of cSMM on PWF and Hydraulic Resistance of CA Membranes

The PWF of compacted CA and CA/cSMM membranes was measured at a constant sampling period under steady state conditions, after 30-40 min of stabilization at 345 kPa. The influences of cSMM additive content in the casting solution of CA and cSMM on the PWF of the blend membranes are given in Table 1. The pure CA (100%) membrane, exhibited a low value of 21.6 lm^{-2} h^{-1} as PWF due to its crystalline nature. As the cSMM content in the casting solution was increased from 0 to 1 wt%, an increase of flux from 21.61 to 24.94 lm^{-2} h^{-1}. This improvement in flux may be due to the increase in hydrophilic nature of blend membranes due to addition of hydrophilic cSMM in blend membranes. Similar in flux up to 83.74 lm^{-2} h^{-1} was also observed when the cSMM content was in-

Table 1. Performance of the CA/cSMM blend membranes

Blend composition, wt%		Solvent, wt%	PWF	R_m	%SR	MWCO
CA	cSMM	NMP	($lm^{-2}h^{-1}$)	($kPa/lm^{-2}h^{-1}$)		(kDa)
17.5	0	82.5	21.61	13.89	83.1	20
17.5	1	81.5	24.94	12.05	82.4	20
17.5	2	80.5	34.90	9.07	80.6	20
17.5	3	79.5	52.36	6.17	80.7	35
17.5	4	78.5	83.74	4.12	84.0	45

creased to 4 wt%. Thus, the increase in flux is a direct consequence of the presence of cSMM in the blend. The increase in flux is not only due to the hydrophilicity but also due to the presence of a sulfonic group in cSMM, leading to the formation of cavities in the sub layer, which gives way to the mobility of the water molecules [43].

From the experimental data in Table 1, it is evident that the pure CA membrane exhibited a higher membrane resistance of 13.89 $kPa/lm^{-2}h^{-1}$ due to its low porosity [44]. However, in the blend membranes, an increase in cSMM additive content from 1 to 4 wt% decreased the hydraulic resistance gradually from 12.05 to 4.12 $kPa/lm^{-2}h^{-1}$. This may be explained by the fact that an increase in the concentration of cSMM enhances the size of pores to a great extent due to larger segmental gap between polymer chains, which leads to the decrease in the value of hydraulic resistance resulting in the formation of macrovoids on the membrane surface due to thermodynamical instability [45].

4. Molecular Weight Cut-off Measurement

The molecular weights of the molecule larger than the molecular weight of a membrane will retain on the membrane. In this investigation, the MWCOs of the membranes determined by UF experiments with BSA, EA, pepsin and trypsin as the protein solutes are shown in Table 1. The solutes generally used are proteins which are considered to be spherical. Since, the MWCO of a particular membrane corresponds to the molecular weight of the proteins having beyond 80% of solute rejection [36]. MWCO depends also on the structure of the permeate species and its three-dimensional structure [46]. Pure CA and 1 wt% and 2 wt% cSMM blend membranes showed an MWCO of 20 kDa because of their smaller pore size. Furthermore, with an increase in cSMM (4 wt%) content in the blend, the percentage solute rejection decreases and the MWCO of the membranes improved significantly (45 kDa) because of the larger pore size of these blend membranes.

5. Protein Rejection and Permeation Study

The solute rejection of these proteins was analyzed for pure CA and modified blend CA membranes and the results are drawn in Fig. 4. The composition of the casting solution plays a crucial role in the separation of proteins. From the rejection values it can be noted that as cSMM additive content increased from 1 to 4 wt% in CA blend membrane, the percentage solute rejection decreased. This may be due to the higher cSMM additive concentration that created the mixed casting solution uneven and inhomogeneity, resulting in the formation of larger pores within the membranes. In addition, the percentage solute rejection is high in small pore membranes, because the electrical repulsion acts more strongly on a charged protein molecule permeating through a smaller pore of a charged membrane [47]. Therefore, it may be concluded that the rejection percentage of pure

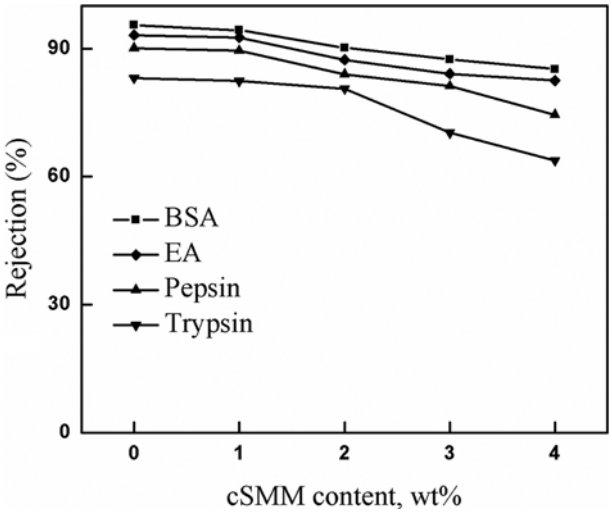

Fig. 4. Protein rejection of the CA/cSMM blend membranes with different cSMM additive composition.

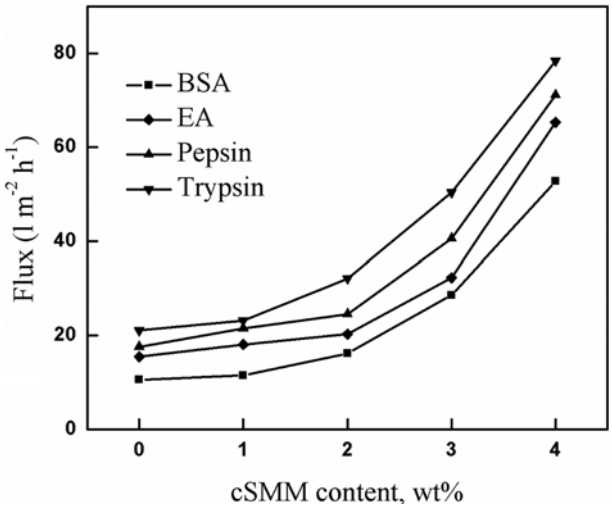

Fig. 5. Protein flux of the CA/cSMM blend membranes with different cSMM additive composition.

CA membrane was much higher than that of cSMM blended CA membranes.

The permeate flux of pure and surface modified CA blend membranes of different proteins was calculated and their flux values are drawn in Fig. 5. From the figure, trypsin had a higher flux than BSA for all blend membranes. The pure CA (100%) membranes showed the permeate flux of 10.56, 15.48, 17.60 and 21.10 $lm^{-2}h^{-1}$ for BSA,

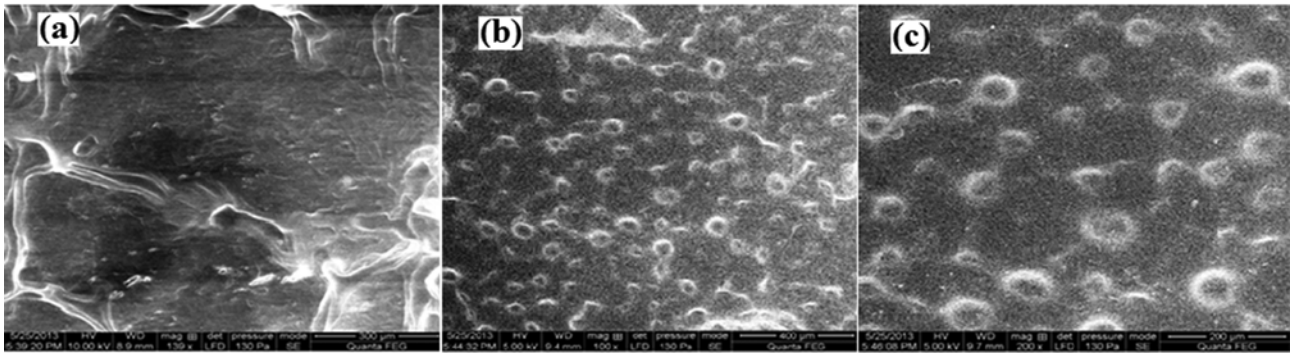

Fig. 6. The SEM micrographs of top surface of CA/cSMM blend membranes with different cSMM additive composition: (a) 0 wt% cSMM, (b) 2 wt% cSMM, (c) 4 wt% cSMM.

EA, pepsin and trypsin, respectively. Furthermore, the 4 wt% of cSMM additive content in the blend CA membrane, the permeate protein flux increased to 52.74, 65.31, 71.12, and 78.47 $lm^{-2}h^{-1}$ at BSA, EA, pepsin and trypsin, respectively. Trypsin had a higher permeation rate than that of all other proteins studied. The order of permeate flux was found to be BSA<EA<pepsin<trypsin. The reason for this trend may be due to the sieving size of the different proteins such as trypsin, pepsin, EA and BSA of 20 kDa, 35 kDa, 45 kDa and 69 kDa, respectively.

6. Effect of cSMM on Surface Characteristics of CA Membranes

An SEM was employed to observe the top surface of the membranes. Fig. 6(a) shows that in the absence of cSMM additive in CA the membrane pore size is very small and there is a notable increase in the pore size of the membrane from the CA to the CA/cSMM blend membrane, indicating an increase in free volume that can be associated with the intake of water molecules [48].

WC is correlated with hydrophilicity of the membrane [49]. The WC of CA/cSMM membranes at various compositions are given in Table 2. The WC of the membranes was increased with an increasing of cSMM in the casting solution. The pure CA membrane has lower WC of 66.5%. The addition of hydrophilic cSMM in the casting solution resulted in blend membrane with 4 wt% and the WC was found to be 79.6%. Thus, for higher WC this may be due to the additional sulfonic groups from the cSMM additive concentration.

Fig. 7 shows the results of the contact angle measurement. The pure base polymer had a contact angle of 66.2°, indicating to be slightly hydrophilic. After being modified with the additive (cSMM), the membrane became much more hydrophilic, with a contact angle for 1 wt% cSMM at 65.5°, 2 wt% cSMM at 61.0°, 3 wt% cSMM at 52.0° and that for 4 wt% cSMM at 42.4°. The contact angle of CA is higher than CA/cSMM blend membrane. Meanwhile, the adhesion work of cSMM modified blend membranes is higher compared to pure CA membrane as shown in Table 2. The different values of adhesion work (ω_A) for CA/cSMM blend membranes exhibited their hydrophilicity. Both trends of the contact angle and adhesion work indicate the hydrophilicity of the CA/cSMM blend membrane, which increases with the increase of cSMM concentration.

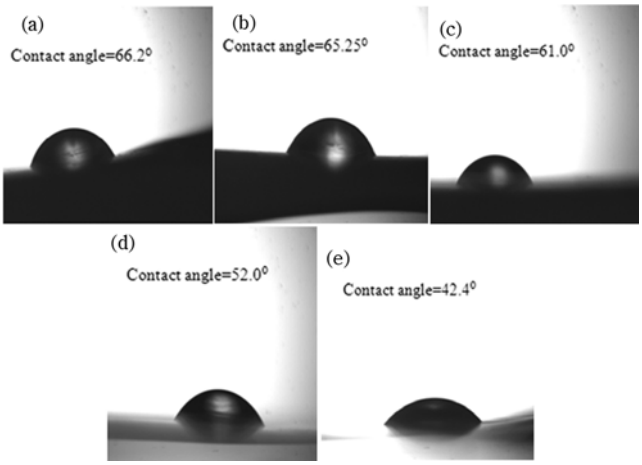

Fig. 7. The contact angle of the CA/cSMM blend membranes: (a) 0 wt% cSMM, (b) 1 wt% cSMM, (c) 2 wt% cSMM, (d) 3 wt% cSMM, (e) 4 wt% cSMM.

The contact angle is correlated with adhesion work and WC. As the contact angle decreases the WC increases and similar increasing trend as observed in adhesion work. This follows the natural

Table 2. Water content, adhesion work, pore radius, porosity of the CA/cSMM blend membranes

Blend composition, wt%		Solvent, wt%	Water content	Adhesion work	Pore radius,	Porosity,
CA	cSMM	NMP	(%)	(mN/m)	R (Å)	ε (%)
17.5	0	82.5	66.5	102	27.68	0.006
17.5	1	81.5	68.3	104	27.91	0.007
17.5	2	80.5	71.2	108	28.54	0.009
17.5	3	79.5	74.0	118	32.71	0.012
17.5	4	78.5	79.6	127	41.26	0.015

behavior as an indication of an increase in hydrophilicity. Considering further that the contact angle and adhesion work is related to the surface, while the WC is a bulk property, the earlier correlation implies that the surface property is affected by the bulk property and vice versa. This is logical considering that the contact angle also depends on the presence of water in the membrane pores and hence on the morphology underneath top surface layer [50].

7. Average Pore Size and Surface Porosity Measurement

The pore size and surface porosity of the virgin CA and surface modified CA blend membranes determined from the protein rejection studies are shown in Table 2. From the table, it is evident that an increase in the cSMM content in the casting solutions led to changes in pore size and porosity. Addition of 1 wt% cSMM into the casting solution induced the formation of bigger pore size. The increase in pore size by the addition of cSMM is due to the formation of clusters of sulfonate ions, into which water droplets are entrapped. This would lead to the increase in the permeation rate of the membrane [51], which is in agreement with the results obtained in this study. Further increasing the cSMM upto 4 wt% resulted in the increase in the pore size and porosity to a maximum of 41.26 Å and 0.015%, respectively. The CA/cSMM blended membranes had a bigger pore size distribution than the pure CA membrane.

8. Effect of cSMM on CA Membranes on Flux Decline Rate, FRR, Internal Membrane Fouling and Surface Fouling Rate

Flux decline rate (R_{fd}) was used to analyze the fouling resistant ability of the membranes. A lower value of R_{fd} means higher anti fouling property of the membranes and vice versa [52]. The flux decline rate of pure CA membrane was found to be 59.4%. The cSMM additive was increased in CA blend membranes from 1 to 4 wt%; the flux decline rate values are 54.0%, 53.5%, 51.0% and 47.2%, respectively. as shown in Fig. 8(a). From the figure it was observed that when the cSMM additive concentration in the casting solution was increased, the flux decline rate was decreased to a significant level due to the higher sulfonated content of cSMM, which enhances the hydrophilicity and reduces the BSA adsorption into the membrane pores as a results decrease in flux decline rate.

Membrane fouling could reduce the permeation efficiency and restrict the wide application of UF membrane. Membrane cleaning is often used to recover flux, and FRR value is introduced to evaluate membrane antifouling property: the capability of antifouling property is more effective, the higher FRR value is obtained [53]. The FRR of pure CA membrane showed a result of 66.12%. and the cSMM content increased upto 4 wt%, the FRR values are 73.34%, 79%, 85% and 89%, respectively, as shown in Fig. 8(b). The increase in the FRR with the cSMM content could be explained by the fact that an increase in the content of cSMM results in increasing hydrophilicity of membrane, which leads to decrease in protein adsorption. The increasing hydrophilicity of membranes weakened the interaction between membrane surface and proteins, because protein and many other foulants are hydrophobic in nature [54]. So that protein foulants can be easily washed away from the modified membranes. As result, flux recovery was higher, which indicates that the surface modified membranes have better fouling resistance behavior.

Meanwhile, the fouling resistant characteristic of internal membrane fouling (irreversible) and surface fouling (reversible) flux rate of the pure CA and CA/cSMM blend membranes were measured. The internal membrane fouling of pure CA membrane was 34%; when the cSMM content increased up to 4 wt% the values decreased to 11%, as shown in Fig. 8(c). It was observed that the internal membrane fouling rate of the pure CA membrane was higher than that of CA/cSMM modified blend membranes and main flux decline was because of irreversible fouling. From this it was noted that CA/cSMM blend membranes have a better ability to resist the membrane fouling than pure CA membrane due to the presence of sulfonate groups on the membrane surface. The existence of sulfonate groups in cSMM on the CA membrane surface enhanced the hydrophilicity and further reduced proteins adsorption and deposition [55]. The surface fouling rate of pure CA membrane has the value of 25.5% as shown in Fig. 8(d). The cSMM modified CA membranes of the surface fouling rate increased to 34%, which can be easily washed out by simple hydraulic cleaning.

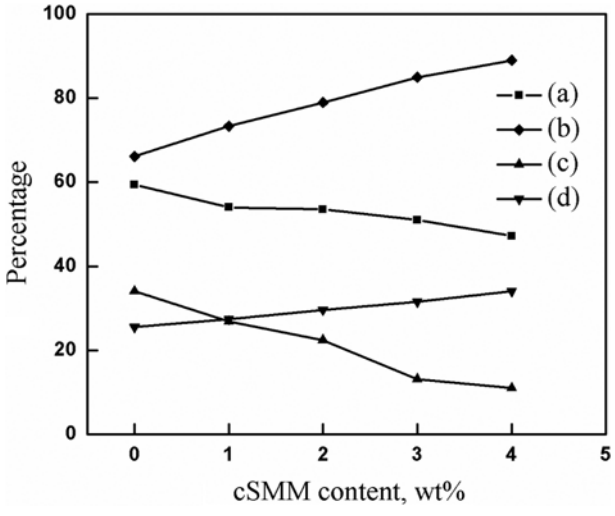

Fig. 8. Effect of cSMM on anti-fouling characteristics of CA membranes.
(a) Flux decline rate, (b) Flux recovery ratio, (c) Internal membrane fouling rate, (d) Surface fouling rate

CONCLUSIONS

The synthesized cSMM contains charged sulfonic groups, and it was confirmed by FT-IR spectroscopy. The prepared cSMM was blended into the casting solution of CA with different composition by phase inversion technique. SEM and contact angle study explained that the promoting additive content of cSMM led to an increase in pore size and surface hydrophilicity of the membrane, which results in higher PWF and WC in blend membranes. As the content of cSMM increases in cSMM blended membrane the average pore size, porosity and MWCO value increase significantly. Hydrophilic surface treatment results of cSMM segments resist the protein adsorption at the membrane surfaces effectively, resulting in enhanced antifouling properties such as reduction in flux decline rate and irreversible fouling rate, increase in FRR and reversible fouling rate during the foulant solution of protein separation processes. From these observations, we conclude that blending hydrophilic nature of cSMM into the CA membrane increases the performance of UF membrane, indicating the charged surface modified CA blend membrane, which plays a significant role in reforming permeation and

fouling resistant propensity characteristics.

ACKNOWLEDGEMENTS

This work was supported by the Science and Engineering Research Board (SERB), Department of Science and Technology, Government of India under the project number SR/FT/CS-22-2011. This support is gratefully acknowledged.

REFERENCES

1. V. A. K. Anthati and K. V. Marathe, *Can. J. Chem. Eng.*, **89**, 292 (2011).
2. C. Azoug, Z. Sadaoui, F. Charbit and G. Charbit, *Can. J. Chem. Eng.*, **75**, 74 (1997).
3. C. F. Lin, C. H. Wu and H. T. Lai, *Sep. Purif. Technol.*, **60**, 292 (2008).
4. W. Yuan and A. L. Zydney, *J. Membr. Sci.*, **157**, 1 (1999).
5. C. W. Jung and L. S. Kang, *Korean J. Chem. Eng.*, **20**, 855 (2003).
6. O. Kuttowy and S. Sourirajan, *J. Appl. Polym. Sci.*, **19**, 1449 (1975).
7. R. Haddada, E. Ferjani, M. S. Roudesli and A. Deratani, *Desalination*, **167**, 403 (2004).
8. P. Maheswari and D. Mohan, *High Perform. Polym.*, **25**, 641 (2013).
9. H. T. Yeo, S. T. Lee and M. J. Han, *J. Chem. Eng. Japan*, **33**, 180 (2003).
10. D. B. M. Jimenez, R. M. Narbaitz, T. Matsuura, G. Chowdhury, G. Pleizier and J. P. Santerre , *J. Membr. Sci.*, **231**, 209 (2004).
11. A. Nagendran and D. Mohan, *Polym. Adv. Technol.*, **19**, 24 (2008).
12. A. Idris, N. M. Zain and M. Y. Noordin, *Desalination*, **207**, 324 (2007).
13. N. A. Ochoa, M. Masuelli and J. Marchese, *J. Membr. Sci.*, **278**, 457 (2006).
14. A. V. R. Reddy, D. J. Mohan, P. R. Buch, S. V. Joshi and P. K. Ghosh, *Int. J. Nucl. Desalination*, **2**, 103 (2006).
15. D. L. Cho, S. H. Kim, Y. H. Huh, D. Kim, S. Y. Cho and B. H. Kim, *Macromol. Res.*, **12**, 553 (2004).
16. D. E. Suk, G. Chowdhury, T. Matsurra, R. M. Narbaitz, P. Santerre, G. Pleizier and Y. Deslandes, *Macromolecules*, **35**, 3017 (2002).
17. D. Rana, T. Matsuura, R. M. Narbaitz and C. Feng, *J. Membr. Sci.*, **249**, 103 (2005).
18. D. Rana, B. Scheier, R. M. Narbaitz, T. Matsuura, S. Tabe, S. Y. Jasim and K. C. Khulbe, *J. Membr. Sci.*, **409-410**, 346 (2012).
19. D. Rana, Y. Kim, T. Matsuura and H. A. Arafat, *J. Membr. Sci.*, **367**, 110 (2011).
20 D. E. Suk, T. Matsuura, H. B. Park and Y. M. Lee, *J. Membr. Sci.*, **277**, 177 (2006).
21. D. Rana, T. Matsuura and R. M. Narbaitz, *J. Membr. Sci.*, **282**, 205 (2006).
22. Y. Fang, V. H. Pham, T. Matsuura, J. P. Santerre and R. M. Narbaitz, *J. Appl. Polym. Sci.*, **54**, 1937 (1994).
23. Y. Kim, D. Rana, T. Matsuura and W.-J. Chung, *Chem. Commun.*, **48**, 693 (2012).
24. M. N. A. Mohd Norddin, D. Rana, A. F. Ismail, T. Matsuura, R. Sudirman and J. Jaafar, *J. Ind. Eng. Chem.*, **18**, 2016 (2012).
25. A. Hamza, V. A. Pham, T. Matsuura and J. P. Santerre, *J. Membr. Sci.*, **131**, 217 (1997).
26. N. Bolong, A. F. Ismail, M. R. Salim, D. Rana, T. Matsuura, A. Tabe-Mohammadi, *Sep. Purif. Technol.*, **73**, 92 (2010).
27. M. N. A. Mohd Norddin, A. F. Ismail, D. Rana, T. Matsuura, A. Mustafa and A. Tabe-Mohammadi, *J. Membr. Sci.*, **323**, 404 (2008).
28. P. S. T. Machado, A. C. Habert and C. P. Borges, *J. Membr. Sci.*, **155**, 171 (1999).
29. C. Barth, M. C. Gonclaves, A. T. N. Pires, J. Roeder and B. A. Wolf, *J. Membr. Sci.*, **169**, 287 (2000).
30. G. Arthanareeswaran, K. Srinivasan, R. Mahendran, D. Mohan, M. Rajendran and V. Mohan, *Eur. Polym. J.*, **4**, 751 (2004).
31. D. Bhattacharya, J. M. McCarthy and R. B. Grieves, *AIChE J.*, **20**, 1206 (1974).
32. M. Tamura, T. Uragami and M. Sugihara, *Polymer*, **22**, 829 (1981).
33. R. Mahendran, R. Malaisamy and D. Mohan, *Polym. Adv. Technol.*, **15**, 149 (2004).
34. M. Sivakumar, R. Malaisamy, C. J. Sujatha, D. Mohan, V. Mohan and R. Rangarajan, *J. Membr. Sci.*, **169**, 215 (2000).
35. S. P. Nunes and K. V. Peinemann, *J. Membr. Sci.*, **73**, 25 (1992).
36. M. N. Sarbolouki, *Sep. Sci. Technol.*, **17**, 381 (1982).
37. O. Velicangil and J. A. Howell, *J. Phys. Chem.*, **84**, 2991 (1980).
38. Y. Q. Wang, Y. L. Su, X. L. Ma, Q. Sun and Z. Y. Jiang, *J. Membr. Sci.*, **283**, 440 (2006).
39. A. Jayalakshmi, S. Rajesh and D. Mohan, *Appl. Surf. Sci.*, **258**, 9770 (2012).
40. R. W. Baker, *Membrane technology and applications*, Wiley, Chichester, UK (2004).
41. V. Gekas, *Desalination*, **68**, 77 (1988).
42. L. Brinkert, N. Abidine and P. Aptel, *J. Membr. Sci.*, **77**, 123 (1993).
43. C. L. Brousse, R. Chapurlat and J. P. Quentin, *Desalination*, **18**, 137 (1976).
44. G. Arthanareeswaran, C. S. Latha, D. Mohan, M. Rajenthiren and K. Srinivasan, *Sep. Sci. Technol.*, **41**, 2895 (2006).
45. M. Ousman and M. Bennasar, *J. Membr. Sci.*, **105**, 1 (1995).
46. A. S. Michaels, L. Nelsen and M. C. Porter, *Ultrafiltration in membrane processes in industry and biomedicine*, Plenum Press, New York (1971).
47. S. Nakao, H. Osada, H. Kurata, T. Tsuru and S. Kimura, *Desalination*, **70**, 191 (1988).
48. M. N. A. Mohd Norddin, A. F. Ismail, T. Matsuura and D. Rana, *J. Teknol.*, **49**, 91 (2008).
49. M. Sivakumar, D. Mohan and R. Rangarajan, *J. Membr. Sci.*, **268**, 208 (2006).
50. Y. X. Ma, F. G. Shi, J. Ma, M. N. Wu, J. Zhang and C. J. Gao, *Desalination*, **272**, 51 (2011).
51. Y. Kim, D. Rana, T. Matsuura and W. J. Chung, *J. Membr. Sci.*, **338**, 84 (2009).
52. A. Nagendran and D. Mohan, *J. Appl. Polym. Sci.*, **110**, 2047 (2008).
53. A. Nagendran, A. Vijayalakshmi, D. Lawrence Arockiasamy, K. H. Shobana and D. Mohan, *J. Hazard. Mater.*, **155**, 477 (2008).
54. D. Rana and T. Matsurra, *Chemical Reviews*, **110**, 2448 (2010).
55. J. S. Taurozzi, C. A. Crock and V. V. Tarabara, *Desalination*, **269**, 111 (2011).